

Experimental study on two types of new beam-to-column connections

Hongwei Ma^{1,2*} Weishan Jiang³ and Chongdu Cho⁴

¹*State Key Laboratory of Subtropical Architecture Science, South China University of Technology, Guangzhou, PR China*

²*School of Civil Engineering and Transportation, South China University of Technology, Guangzhou, PR China*

³*School of Civil Engineering, Xi'an University of Architecture & Technology, Xi'an, PR China*

⁴*Department of Mechanical Engineering, Inha University, Yong-hyun Dong 253, Incheon, S. Korea*

(Received December 04, 2009, Accepted June 21, 2011)

Abstract. The new structure consisting of continuous compound spiral hoop reinforced concrete (CCSHRC) column and steel concrete composite (SCC) beam has both the advantages of steel structures and concrete structures. Two types of beam-to-column connections applied in this structural system are presented in this paper. The connection details are as follows: the main bars in beam concrete pass through the core zone for both types of connections. For connecting bar connection, the steel I-beam webs are connected by bolts to a steel plate passing through the joint while the top and bottom flanges of the beams are connected by four straight and two X-shaped bars. For bolted end-plate connection, the steel I-beam webs are connected by stiffened extended end-plates and eight long shank bolts passing through the core zone. In order to study the seismic behaviour and failure mechanisms of the connections, quasi-static tests were conducted on both types of full-scale connection subassemblies and core zone specimens. The load-drift hysteresis loops show a plateau for the connecting bar connection while they are excellent plump for bolted end-plate connection. The shear capacity formulas of both types of connections are presented and the values calculated by the formula agree well with the test results.

Keywords: beam-to-column connection; X-shaped bar; seismic behaviour; quasi-static test; shear capacity; ductility

1. Introduction

Reinforced concrete steel (RCS) moment frame consisting of reinforced concrete (RC) columns and steel (S) beams attracts attentions for seismic resistant design of structures. Since RC columns possess excellent stiffness and steel beams have good ductility, a properly designed RCS frame has good seismic behaviour and is more economical than the solely steel or RC moment frames. As an innovative hybrid structure, RCS frame was the main part of structures studied in the fifth phase of the United States-Japan Cooperative Research in Urban Earthquake Disaster Mitigation (Deierlein and Noguchi 2004, Goel 2004). However, in order to take full advantage of the good seismic behaviour of RCS moment frames, the beam-to-column connections within the frames must be properly designed and detailed because

* Corresponding author, Associate Professor, E-mail: hwma@scut.edu.cn

the connection configurations, strength, ductility, yielding mechanisms and failure mode would significantly affect the behaviour of RCS frames (Choi and Lee *et al.* 2010). For the RCS frame beam-to-column connections with beam continuously passing through the core zones (also referred to as beam-through-type), they can have good strength and stiffness (Cheng and Chen 2005). These connections behave in a ductile manner when special configurations, such as steel band plates or face bearing plates for interior and exterior connections (Cheng and Chen 2005, Liang and Parra-Montesinos 2004, Parra-Montesinos and Wight 2000) and enough anchorage length of column longitudinal bars for roof level T-connections (Fargier-Gabaldon and Parra-Montesinos 2006), are adopted to prevent shear yielding and bearing failure of column concrete. With considering the floor slab effects, the connections may exhibit not only desirable deformation capability (Bugeja *et al.* 2000), but also an increased beam strength when the interstorey drift angle is below a certain value (Liang and Parra-Montesinos 2004, Liu and Astaneh-Asl 2000). Meanwhile, for the connections with beam flanges interrupted at the core zones (also referred to as column-through-type), they have minimum impact on the column reinforcing bar arrangement and accord with a strong column-weak beam design philosophy. To ensure reliable seismic performance of the column-through-type connections, additional effort in connection details is needed. Numerous details of column-through-type connections have been proposed and investigated in Japan (Architectural Institute of Japan 2001), the results indicate that proper structural configurations of the connections, such as thickening cover plates and face bearing plates, would ensure that the connections have reliable mechanical behaviour (Deierlein and Noguchi 2004, Kuramoto and Nishiyama 2004). Recent development of deformation based design methodology of RCS connections, which can effectively control the distortions and damages of the connections, has been presented by Parra-Montesinos (Parra-Montesinos *et al.* 2003). The behaviour of RCS frames has been studied either by finite element method (Noguchi and Uchida 2004) or by analytical analysis (Cheng and Chen 2005), and the seismic design guidelines for this new structure system were already proposed by (Architectural Institute of Japan 2000, Bracci *et al.* 1999, Nishiyama *et al.* 2004).

Recently, a new type of RC columns, namely, continuous compound spiral hoop reinforced concrete column (CCSHRC column) has been proposed to be used in moment frames. Since the transverse reinforcement is deeply enhanced, the CCSHRC column consists of a core zone with fully confined concrete by continuous compound spiral hoop as shown in Fig. 1. High volumetric ratio of transverse reinforcement is apparent. Moreover, the cold drawn low carbon steel wire with a tensile strength ranging from 335~1570 N/mm² can be used as the stirrup of CCSHRC column, so it is easy to obtain an ideal confinement effect on core zone concrete (Han 2002). CCSHRC column has the same performance as concrete filled steel tube (CFT) column. Test results from both previous studies (Jiang and Bai 1994)

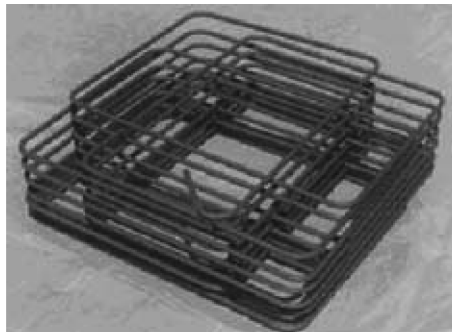


Fig. 1 Continuous compound spiral hoop proposed by Shibata *et al*

and related researches (Binici 2005, Hwang and Yun 2004, Xiao and Martirosyan 1998) indicated that CCSHRC columns can have high strength, good ductility and excellent fire resistance. A new type of hybrid structural system consisting of steel concrete composite (SCC) beams and CCSHRC columns apparently has better structural performance than that of RCS frames.

Similar to the RCS frames, the performance of the SCC beams-CCSHRC columns frames is significantly influenced by the design and details of the beam-to-column connections. However, it is found that much of the previous research works focused only on either the study of the SCC beams or the CCSHRC columns. Hence, a research project was initiated to develop new beam-to-column connections suitable to be used in a moment frame consisting of SCC beams and CCSHRC columns. In order to assess the seismic behaviour and failure mechanisms of the new connections, quasi-static tests have been carried out on both full-scale SCC beam and CCSHRC column subassemblies and core zone specimens. The test results would provide a better understanding of the shear capacity and hysteresis behaviour of the new connections. Moreover, the test results are used to validate whether or not the desired failure modes could occur when they are designed according to the conventional codes for the full-scale connection specimens.

2. Connection configurations

The proposed beam-to-column connections for the SCC beam and CCSHRC column subassemblies, which are column-through-type connections, are shown in Fig. 2. For both types of connections, the steel I-beams are interrupted at the joint while the main bars in beam concrete pass through the core zone. In addition, normal stirrups in the column are replaced by a steel plate hoop and the column main

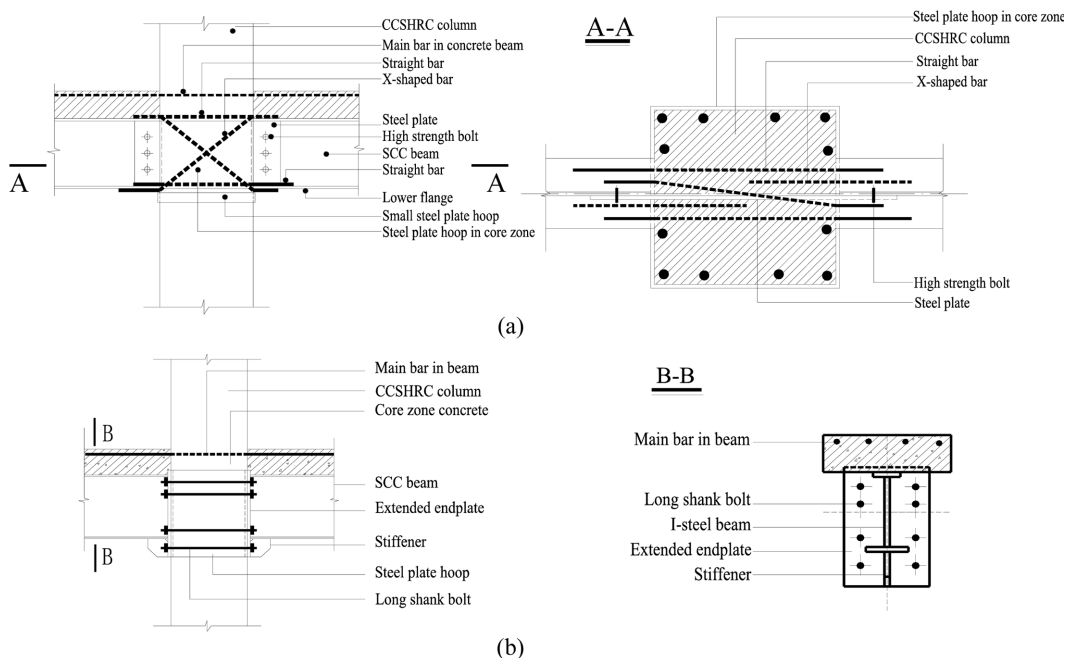


Fig. 2 The configurations for: (a) connecting bar connection, (b) bolted end-plate connection

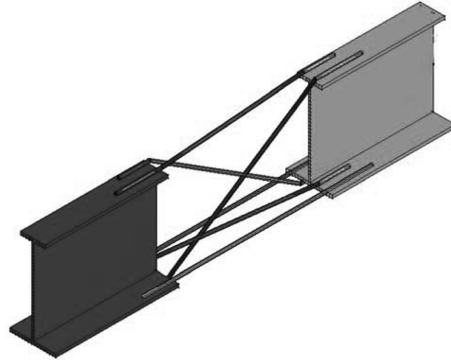


Fig. 3 The details for connecting bar at core zone the core zone

bar arrangement is kept unchanged in the core zone. For connecting bar connection, the steel I-beam webs are connected by bolts to a steel plate passing through the joint while the top and bottom flanges of the beams are connected by four straight and two X-shaped inclined bars using fillet welds, as shown in Fig. 2(a) and 3. In order to alleviate stress concentrations at the welds, different welding lengths for the connecting bars are adopted. For bolted end-plate connection, the steel I-beam webs are connected by two stiffened extended end-plates and eight long shank bolts passing through the core zone. The stiffeners are used to alleviate the stress concentrations and avoid opening of the welds connecting endplate with beam.

According to Kanno and Deierlein (2000), the failure modes of RCS connections can be panel shear yielding, bearing failure and longitudinal reinforcement bond failure. For the proposed connecting bar connection, the core zone is subjected to a shear force under a seismic event (Hadianfard and Rahnema 2010), as shown in Fig. 4. The X-shaped bars are effective in transferring such shear force (Shibata *et al.* 1992). The continuity plate also contributes to the shear capacity of the core zone. All these components prevent the shear failure of the core zone together. The steel plate hoop can protect the column main bars from the bond failure. At the beam-to-column interface near the bottom flange of the beam, a small

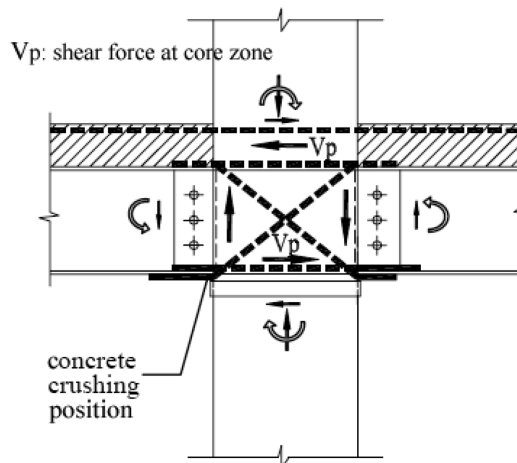


Fig. 4 Distribution of shear forces in the core zone

steel plate hoop is used to prevent the local concrete compressive failure, as shown in Fig. 2. For the bolted end-plate connection, it is convenient to pour core zone concrete when constructing connection in site and the force transmission is smoother with less stress concentrations contrasting to the welded steel connection.

3. Experimental program

3.1. Specimens

Three full-scale beam-to-column subassemblies and three core zone specimens were selected for the experimental study, as shown in Fig. 5. The subassemblies represent an interior moment connection in a SCC beams-CCSHRC columns frame. Both types of full scale connection subassemblies have same dimensions, and they were designed following a strong column and connection - weak beam design philosophy according to the Chinese standard GB50011 (2001). Therefore, for the full-scale connection subassemblies, the core zone was stronger than the adjoining members and shear failure of the core zone would not occur when subjected to a lateral load. For the core zone specimens, they were designed and tested in order to examine the shear capacity. For a beam-to-column connection in the real conditions, the desired failure mode is to force a plastic hinge to form in the beam away from the column face rather than the occurrence of brittle failure in the core zone connection. The test objectives are to validate whether or not the desired failure mode could occur when they are designed according to the conventional codes for the full scale connection subassemblies while to offer data for shear capacity design formula for the core zone specimens.

The geometrical dimensions and reinforcement details of both the full scale connection subassemblies and core zone specimens are illustrated in Fig. 5 and listed in Table 1, respectively. For both types of

Table 1 Geometrical properties and configurations of connection specimens

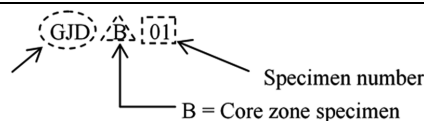
Specimen label ^a	CCSHRC column		SCC beam			Core zone			
	Section dimension (mm)	Reinforcement ratio (%)	I-steel dimension (mm)	Concrete dimension (mm)	X-shaped/straight bars (mm)	Steel plate (mm)	End plate (mm)	Steel plate hoop (mm)	Bolt diameter (mm)
GJD01	400 × 400	3.68	I150 × 80 × 10 × 6	150 × 480	2φ25/4φ25	-700 × 150 × 4	-	430 × 430 × 4	3M22
GJD02	400 × 400	3.68	I150 × 80 × 10 × 6	150 × 480	2φ25/4φ25	-700 × 150 × 4	-	430 × 430 × 4	3M22
LJD01	400 × 400	3.68	I150 × 80 × 10 × 6	150 × 480	2φ25/4φ25	-	-430 × 290 × 32	430 × 430 × 4	8M30
GJDB01	150 × 150	2.01	-	-	2φ12/-	-	-	150 × 150 × 4	-
GJDB02	150 × 150	2.01	-	-	2φ12/-	-	-	150 × 150 × 4	-
LJDB01	150 × 150	2.01	-	-	-	-	-	150 × 150 × 4	4M20

Note: Specimen designations:

Connection type:

GJD = Connecting bar connection

LJD = Bolted end-plate connection



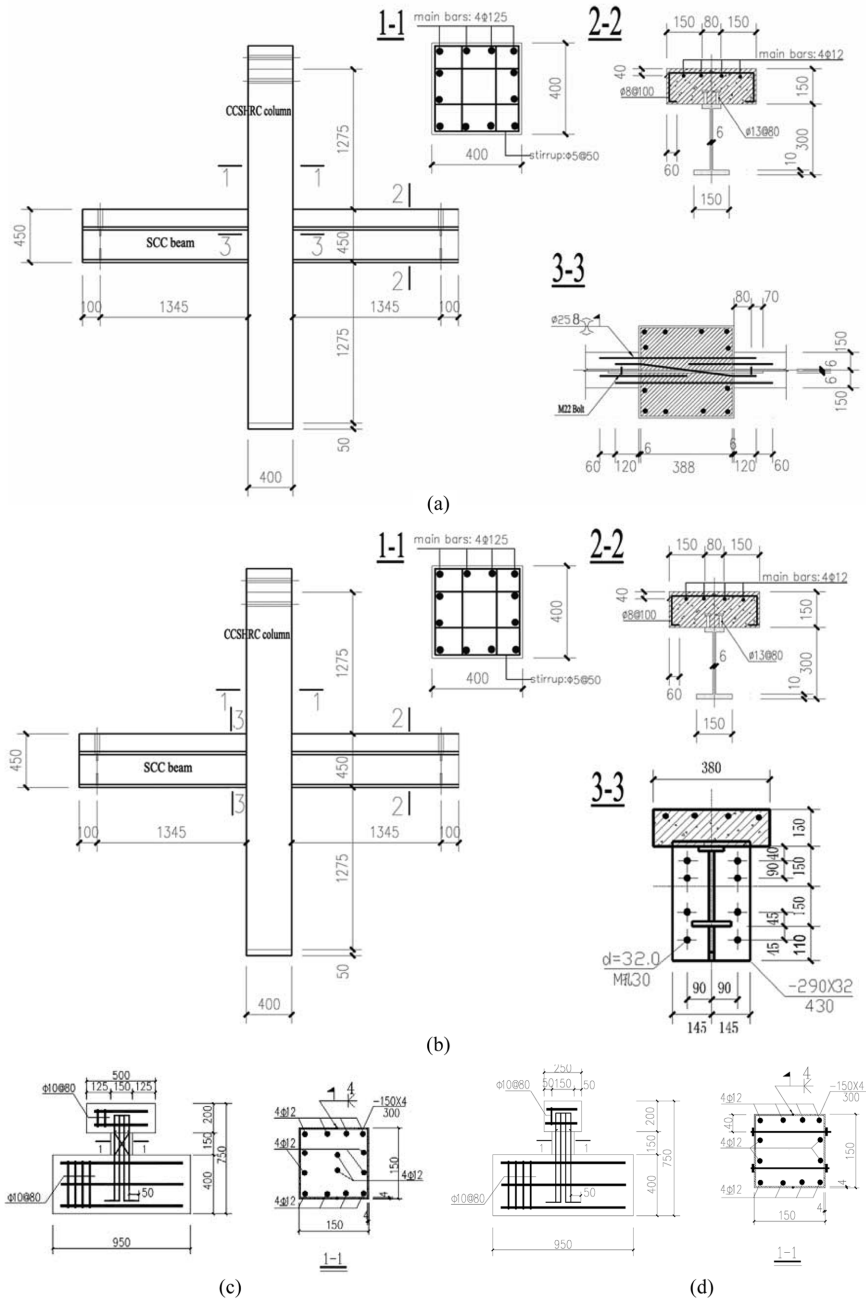


Fig. 5 Geometrical features and reinforcement details of: (a) full-scale connecting bar connection, (b) full-scale bolted end-plate connection, (c) core zone specimen for connecting bar connection, (d) core zone specimen for bolted end-plate connection

full scale connection subassemblies, each SCC beam-tip was at a distance of 1,645 mm from the centreline of the CCSHRC column, as shown in Fig. 5(a) and 5(b), and the height of column was 3,250 mm with pinned boundary conditions. The SCC beam had four 12 mm diameter bars on the top of the cross section

while the CCSHRC column included twelve 25 mm diameter main bars (3.7% reinforcement ratio) arranged symmetrically along the perimeter. The stirrups in the beam consisted of double legs of 8 mm diameter bars spaced 100 mm apart. Concrete slab was connected to steel I-beam by two 13 mm diameter studs that had a mean height of 80 mm and were spaced at 80 mm. The continuous compound spiral hoop in the column consisted six legs of 5 mm diameter steel wires with 60 mm spacing (1.0% reinforcement ratio), as shown in Fig. 5(a) and 5(b). The test results for the steel and reinforcements materials are summarized in Table 2. The concrete cube compressive strengths were equal to 39.2 and 23.3 MPa for the column and beam, respectively.

3.2. Test method

The test setup for both types of full scale connection subassemblies is shown in Fig. 6. The top end of the column was connected to a vertical jack capable of rotation through a universal-pin joint and a horizontal hydraulic actuator, while the bottom end was connected to a ball pivot that allowed rotation. The beam ends on both sides of the connection were pinned. Both full scale connection subassemblies were subjected to an axial compression at the top of the column through a steel reaction beam placed on the column top. Then, cyclic loads were applied to the column top by the hydraulic actuator. The force-displacement mixed loading laws were used in the tests (Jiang and Bai 1994), as shown in Fig. 7. Both the yield load and yield displacement are figured out during the test. The process is as follows: When a small load is imposed to the specimens, the connections are remained in elastic state and the force-displacement relationships are linear. With the increase of applied loads, an inflection point occurs and the force-displacement relationships changes to be nonlinear. The connection rigidity decreased at

Table 2 Material properties of steel plates and reinforcements

Specimen	Yield strength (N/mm ²)	Ultimate strength (N/mm ²)	Young's modulus (N/mm ²)
Column stirrup (φ5)	738.8	764.3	1.78 × 10 ⁵
Beam main bar (φ12)	424.6	597.0	1.77 × 10 ⁵
Column main bar (φ25)	415.8	580.9	1.73 × 10 ⁵
Steel plate hoop	327.5	494.9	1.72 × 10 ⁵
Steel beam web	364.5	526.7	1.85 × 10 ⁵
Steel beam flange	308.5	495.6	2.06 × 10 ⁵

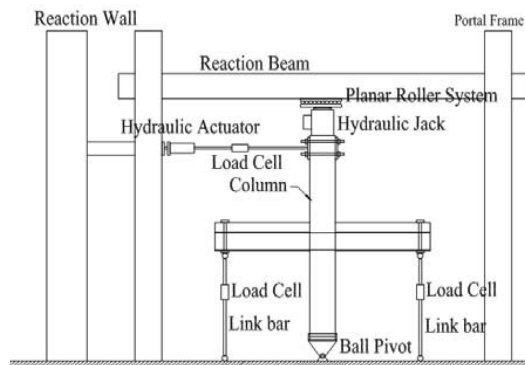


Fig. 6 Test setup for full-scale connection subassembly

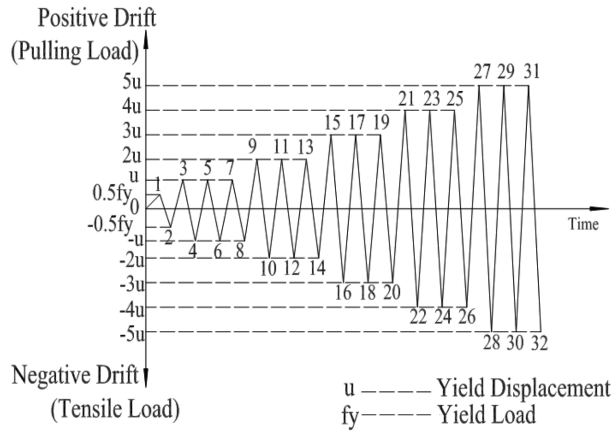


Fig. 7 Loading laws for full scale connection subassembly

abovementioned inflection point, and the corresponding load and displacement are referred to as yield load and yield displacement.

For the core zone specimens, the test setup is shown in Fig. 8. The concrete base of the core zone specimen was fixed to the rigid floor by four threaded rods. The top of the core zone specimens was supported to prevent out-of-plane movement. A constant axial compression load was applied to the column top by a hydraulic jack while the cyclic lateral loads were imposed to the column top by a horizontal hydraulic actuator.

4. Experimental results

4.1. Full-scale connection subassemblies

With an axial compression of 1,200 kN applied to the top of the column and the ratio of axial compressive force to axial compressive ultimate capacity of section maintained at 0.19, the seismic behaviour of specimen GJD01 was studied. When the lateral loads reached 100 kN, cracks perpendicular to the beam axis first appeared at the beam concrete surface. Upon further loading more cracks in the same direction developed. These distributed cracks opened and closed alternatively following the direction of the

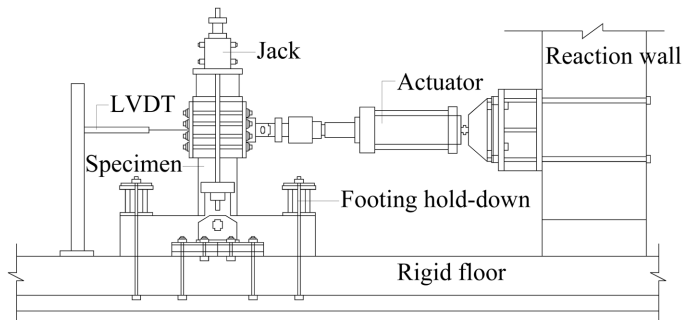


Fig. 8 Test setup for core zone specimen

cyclic loading. When the lateral load reached 125 kN, some hairline thin cracks parallel to the beam axis occurred at the beam concrete surface. During the larger displacement cycles corresponding to 175 kN lateral load, a few shear cracks also emerged at the core zone concrete surface without the steel plate hoop confinement, as shown in Fig. 9(a). Meanwhile, the high strength friction bolts on the steel I-beam webs experienced large slip between the nut and web. During the largest displacement cycles corresponding to 180 kN lateral load, spalling of the concrete covering at the X-shaped bar-lower flange interface (local compressive zone), was observed as shown in Fig. 9(b). The beam concrete near the core zone was crushed and flaked off from the beam surface, and thereby exposing the stirrups as shown in Fig. 9(c). Meanwhile, the beam concrete crack width increased and reached 2-3 mm, and slight buckling of beam lower flanges could be observed. An X-shaped bar fractured due to large tension force while the straight bars together with the welds were able to continue carrying the loads as shown in Fig. 9(d). The test was stopped because of displacement restriction of the horizontal actuator on the column top. Fig. 9(a) shows the physical condition of the connection panel at the end of the tests, it clearly depicts the significantly deteriorated connecting beam. The failure modes and response under lateral loads for specimen GJD02 were similar to those of specimen GJD01, as shown in Fig. 10. It is suggested that more X-shaped bars should be adopted in the core zone with a goal to prevent the fracture of X-shaped bars. Meanwhile, in order to avoid the bond-slip between the straight bars and core zone concrete, short bonding reinforcements should be welded with straight connecting bars with a goal to increase the bond-slip resistance.

For specimen LJD01, two groups of tests were conducted. The connection behaviour was first studied with none axial compression and small lateral cyclic loads applied to the column top. Then, with an axial compression of 1,200 kN applied to the column and the axial compressive ratio maintained at 0.19, the hysteresis behaviour of specimen LJD01 was studied. In the first test, referring to the steel

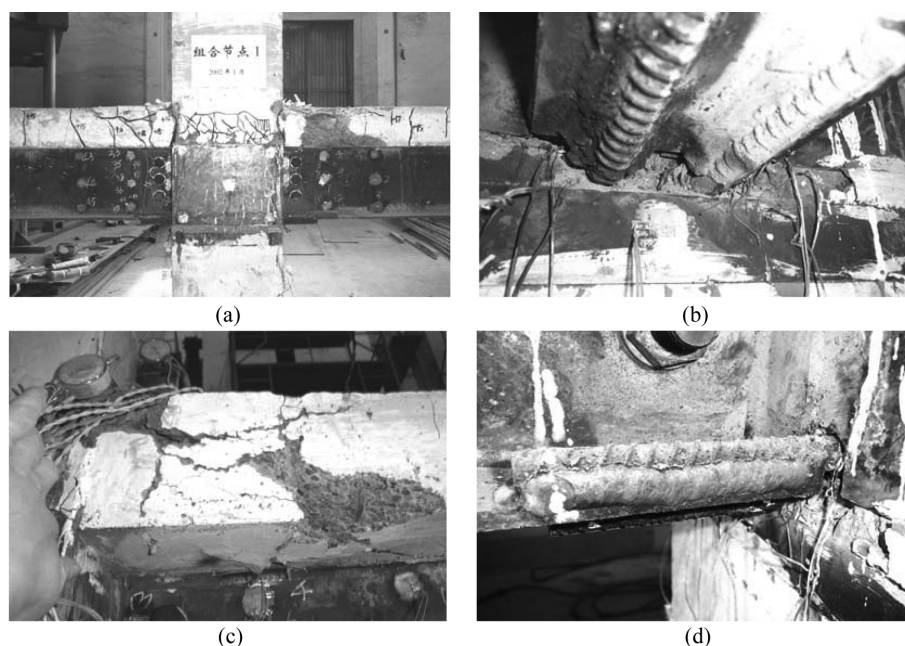


Fig. 9 Specimen GJD01 after test: (a) concrete cracks, (b) local concrete crushing, (c) failure of SCC beam, (d) straight connecting bars and welds

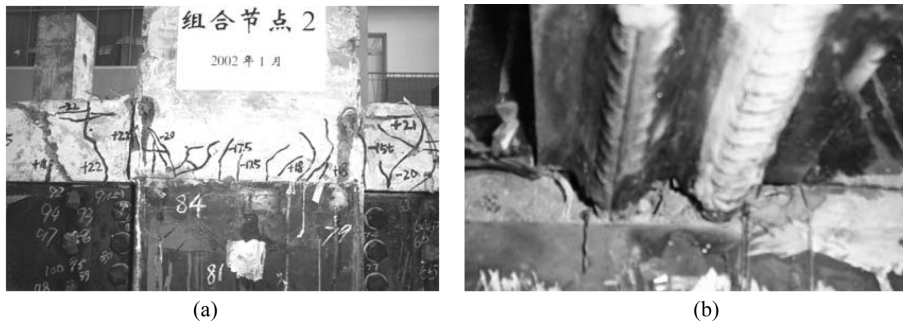


Fig. 10 Specimen GJD02 after test: (a) concrete cracks, (b) failure of the X-shaped bar

beam and concrete column bolted connection tested by Minami (1994), certain pre-tensions were imposed to the long shank bolts with their tensile strains maintained at $200 \mu\epsilon$. When lateral load applied to the column reached 85 kN, the concrete cracks perpendicular to the beam axis occurred at the beam surface, as shown in Fig. 11(a). More cracks occurred with the increase of the lateral loads. During the later loading process, the lower flanges buckled when compressed while recovered to their initial shape when tensioned. In the second test, considering that the core zone concrete was confined by extended end-plate and steel plate hoop, larger pre-tensions were applied to the long shank bolts with the tensile strains in bolt shanks maintained at $800 \mu\epsilon$. When the lateral load applied on the column top reached 180 kN, the lower flange buckled obviously when compressed and recovered to their initial shape when tensioned, as shown in Fig. 11(b) and 11(c). With the lateral load equal to 225 kN, the welds between end-plate and stiffeners cracked. Meanwhile, the crushed concrete massively flaked off from the beam and the beam main bars were exposed as shown in Fig. 11(d), resulting in the unrecoverable deformations of lower flanges when tensioned. Finally, the fracture of lower flange occurred, as shown in Fig. 11(e). The test was stopped because of the displacement restriction of the horizontal actuator. In the test, plastic hinge obviously formed in the beam ends away from the column face. The stiffener effectively alleviated stress concentrations and avoided the cracking of the fillet welds between lower flanges and end-plate. Moreover, the extended end-plate also avoided local compression failure of the core zone concrete.

During the tests of Specimen GJD01 and GJD01, several strain gauges were attached to the X-shaped bars as well as steel I-beam flanges near the core zone to monitor the possible formation of plastic hinges in the beams. Fig. 12 shows the lateral load-strain diagrams for the X-shaped bar, bottom flange and top flange, respectively. It can be seen that the X-shaped bars and top/bottom flanges were all yielded with relatively large strains occurred in the X-shaped bar and the bottom flange. Since lower flange buckling and beam concrete crushing occurred before the fracture of X-shaped bar, it indicated that a plastic hinge developed in the beam end away from the column face.

The curves of lateral loads versus interstory drifts for the full-scale connection subassemblies are shown in Fig. 13. For the connecting bar connections, the former hysteresis loops for both specimens are plump while the latter loops show obvious slipping, as shown in Fig. 13(a) and 13(b). The bond-slip between the straight connecting bars and the core zone concrete cause the horizontal segment in the hysteresis loops. The connection shear capacity consists of the contribution from the increase of beam flexural capacity after the closure of the beam concrete cracks, shear force at the core zone transferred by the steel plate, confinement effect of steel plate hoop, and X-shaped bars. This results in the ascending segment of the hysteresis curves. Meanwhile, for the bolted end-plate connection, in Fig. 13(c) and 13(d) are plotted lateral load and interstory drift relation curves of specimen LJD01 with none and 1,200 kN

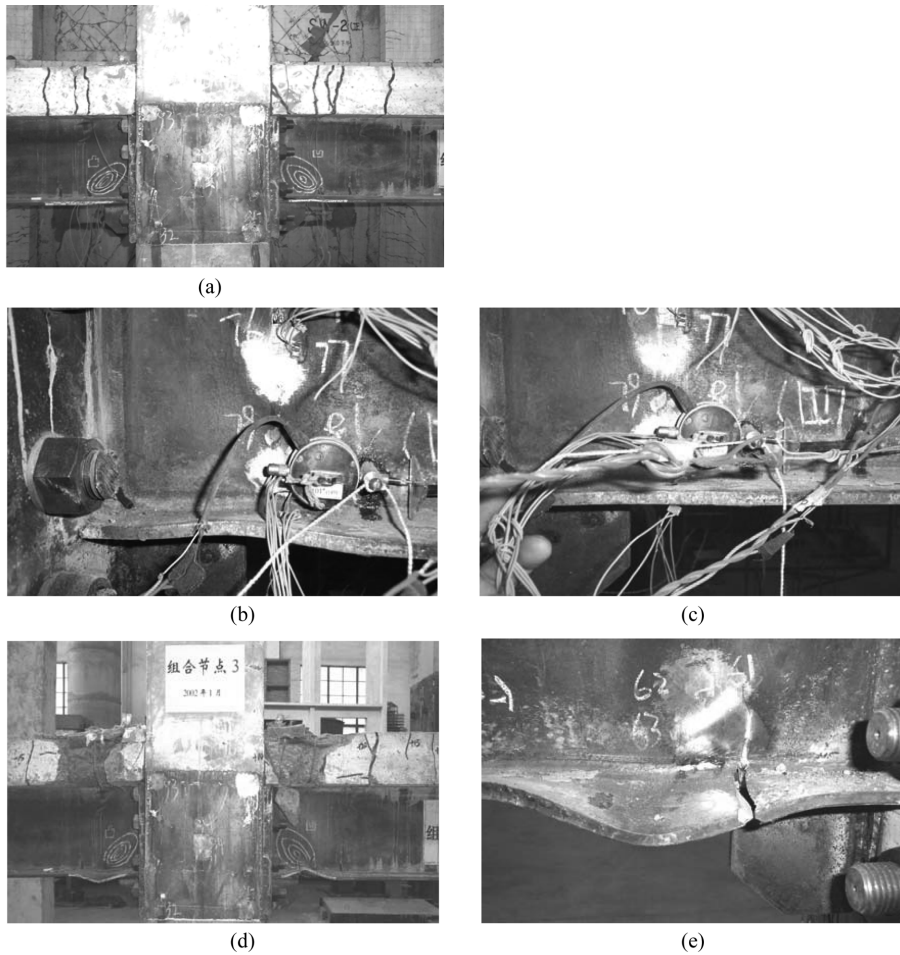


Fig. 11 Specimen LJD01 after test: (a) after the first test, (b) buckling of lower flange, (c) recovering initial shape of lower flange, (d) deformations, (e) fracture of lower flange

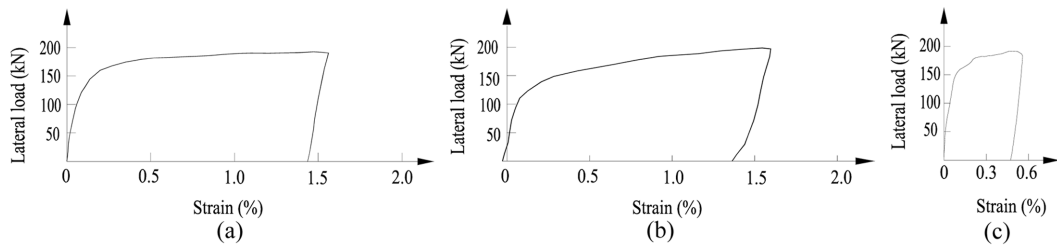


Fig. 12 The load-strain envelope diagram for: (a) X-shaped bar, (b) lower flange, (c) top flange

axial compression applied on column top, respectively. The curves for both tests are plump with slight pinching for the first test while without any slipping and pinching for the second test.

The maximum interstory drift angle for specimens GJD01 and GJD02 reached 0.040 and 0.0385 rad, respectively, while inelastic interstory drift angles for specimen GJD01 and GJD02 equaled to 0.030

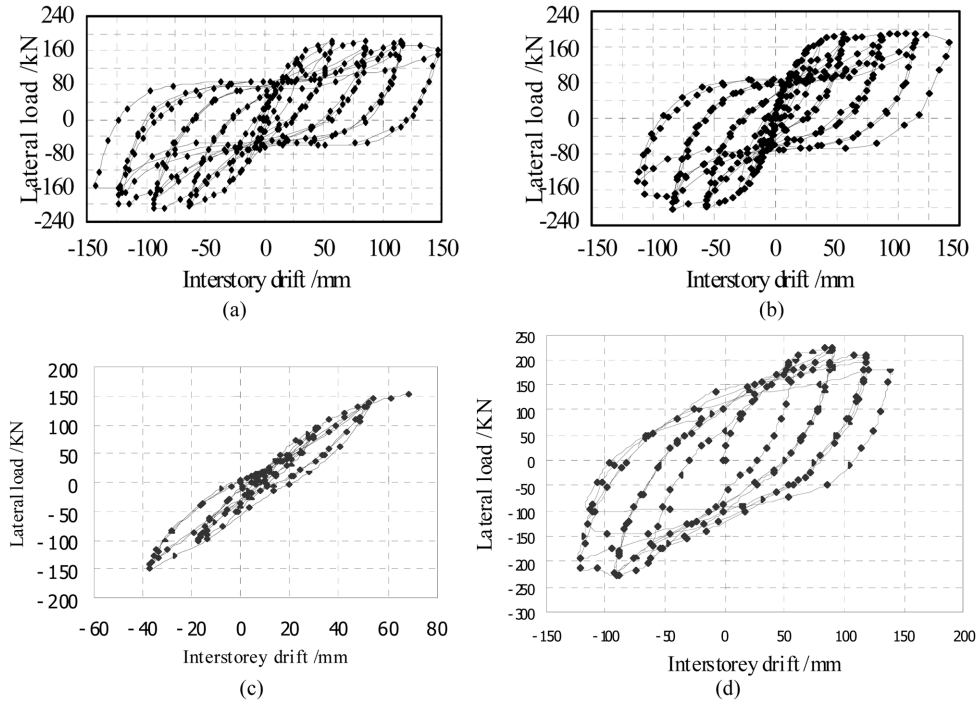


Fig. 13 Lateral load-interstorey drift curves for: (a) specimen GJD01, (b) specimen GJD02, (c) specimen LJD01 without axial compression, (d) specimen LJD01 with axial compression

and 0.032 rad, respectively. The maximum interstorey drift angle for specimen LJD01 reached 0.040 rad, while the inelastic interstorey drift angle equaled to 0.031 rad. Both types of connection specimens developed an inelastic rotation greater than 0.03 rad, as suggested in the AISC Seismic Provisions for Structural Steel Buildings (1997). This indicated that the connection not only had good seismic behaviour but also could be recommended for use in seismic districts.

4.2. Core zone specimens

For both types of core zone specimens, a vertical compression of 800 kN was firstly applied to the specimens and cycle lateral loads were subsequently imposed. All specimens demonstrate same failure modes. All specimens showed an elastic drift with lateral load less than 200 kN. With lateral loads beyond 200 kN, the specimens developed large drifts and steel plate hoop buckled, as shown in Fig. 14. The tests were stopped because the base failures of core zone specimens. Fig. 15 shows the relationships between the lateral loads and drifts for core zone specimens. The hysteresis loops are plump without any pinching and slipping, indicating that the core zone has good energy dissipation capacity. The shear capacity for both specimens does not descend during loading history.

4.3. Shear capacity and configuration proposal

According to the test results and confined concrete theory, the shear capacities for the core zone of both connecting bar and bolted end-plate connections are given by Eq. 1 and Eq. 2, respectively.

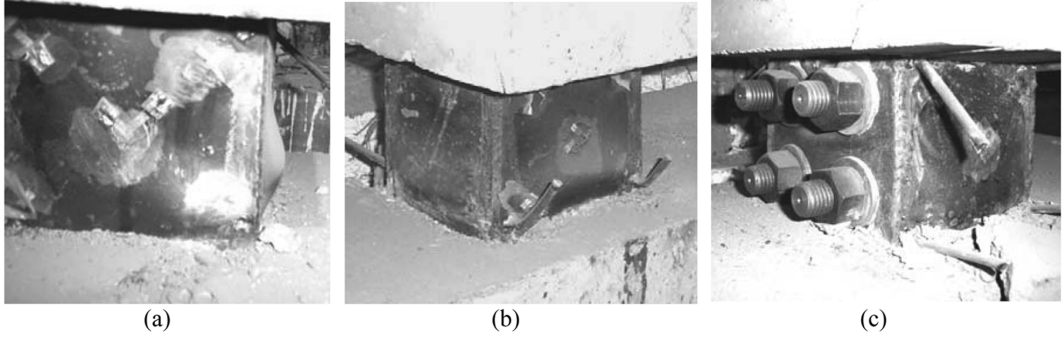


Fig. 14 Core zone specimens after test: (a) specimen GJDB01, (b) specimen GJDB02, (c) specimen LJDB01

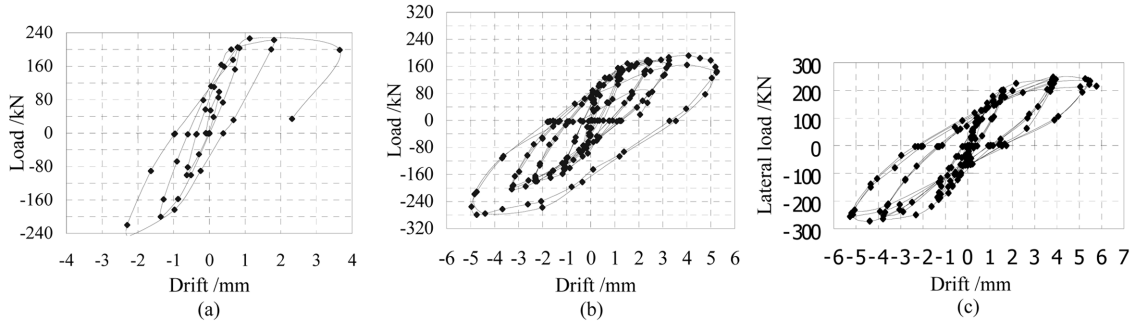


Fig. 15 Lateral load-drift curves for: (a) specimen GJDB01, (b) specimen GJDB02, (c) specimen LJDB01

$$Q_u = 0.1b_jh_jf_{cck} + A_s f_y \cos \theta + \frac{1}{\sqrt{3}} + f_{wy}b_w h_w + 0.056N \quad (1)$$

$$Q_u = 0.15b_jh_jf_{cck} + 0.056N \quad (2)$$

Where b_j is width of core zone; h_j is height of core zone; N is axial compression of column; b_w and h_w are width and height of the steel plate in the core zone, respectively; f_y and f_{wy} are standard yield stress and shear stress for the X-shaped bars and steel plate in the core zone, respectively; A_s and q are cross section area and inclination of the X-shaped bars, respectively; f_{cck} is confined concrete standard compressive strength, which is given by Eq. 3:

$$f_{cck} = \left(1 + \alpha \rho \frac{f_{by}}{f_c}\right) f_c \quad (3)$$

Where ρ is steel plate hoop volume ratio, f_{by} is steel plate hoop standard yield stress, f_c is concrete standard strength, α is confining coefficient, which is equal to 1 and 1.4 for the connecting bar connection and bolted end-plate connection, respectively.

For both types of connection, the test results and calculated values according to Eq. 1 and 2 for the shear capacity of the core zone are listed in Table 3. Two groups of values agree well.

Table 3 Comparison between calculated shear capacity values and test results

Specimen	Calculated values of shear capacity V_C (kN)	Test values of shear capacity V_T (kN)	V_T / V_C
GJD01	1347.1	1251.0	0.93
GJD02	1347.1	1198.2	0.89
LJD01	1441.7	1434.2	1.01
LJDB01	245.4	246.2	1.00
LJDB01	245.4	279.3	1.14
LJDB01	292.2	272.9	1.07

5. Conclusions

This study aims at the new hybrid structure system consisting of SCC beam and CCSHRC column, and presents two types of beam-to-column connections applied in this structure system. The quasi-static tests were carried out on both full-scale connection subassemblies and core zone specimens, and the seismic behaviour and shear capacity of the connections were studied. The primary conclusions can be summarized as follows:

1. The configurations of the proposed connection are feasible and reasonable. For the connecting bar connection, the X-shaped bars, steel plate and confined concrete in the core zone contribute to the shear capacity of the connection. Since the different welding length for the connecting bars at lower flanges was adopted, the weld failures were avoided in the test. For the bolted end-plate connection, it is convenient to pour core zone concrete. The stiffened extended end-plate not only alleviates stress concentrations and avoids the cracking of the fillet welds between lower flanges and end-plate, but also avoids the local compression failures of core zone concrete.
2. For both types of full-scale connection subassemblies, all specimens develop an inelastic rotation greater than 0.03 rad, indicating that the connections are capable of being applied in seismic district. The load-drift hysteresis loops show obvious slipping for the connecting bar connection while are plumb for the bolted end-plate connection.
3. The shear capacity formulas for both types of connections are presented by using confined concrete theory, and the values calculated by the formula agree well with the test results.

Acknowledgement

This study was financially supported by China New Building System Corp. LTD. The authors are grateful to Professor Jiping Hao and Qingrong Yu for their technical supports to the tests of the paper.

References

- American standard, (1997). "Seismic provisions for structural steel buildings." American Institute of Steel Construction, Chicago.
- Architectural Institute of Japan (AIJ). *Design and construction of mixed structures composed of reinforced concrete columns and steel beams*. 2001, Tokyo: Architectural institute of Japan. (in Japanese)
- Binici, B. (2005), "An analytical model for stress-strain behavior of confined concrete." *Eng. Struct.*, **27**(7), 1040-1051.

- Bracci, J.M., Moore, W.P. and Bugeja, M.N. (1999), "Seismic design and constructability of RCS special moment frames." *J. Struct. Eng. ASCE*, **125**(4), 385-392.
- Bugeja, M.N., Bracci, J.M. and Moore, W.P. (2000), "Seismic behavior of composite RCS frame systems." *J. Struct. Eng. ASCE*, **126**(4), 429-436.
- Cheng, C.-T. and Chen, C.-C. (2005), "Seismic behavior of steel beam and reinforced concrete column connections." *J. Constr. Steel Res.*, **61**(5), 587-606.
- Chinese Standard. (2001). "Code for seismic design of buildings (GB50011-2001)." China architectural and building press, Beijing.
- Choi, S.M., Lee, S.H. *et al.* (2010). "Structural characteristics of welded built-up square CFT column-to-beam connections with external diaphragms." *Steel. Comp. Struct.*, **10**(3), 261-279.
- Deierlein, G.G. and Noguchi, H. (2004), "Overview of U.S.-Japan Research on the Seismic Design of Composite Reinforced Concrete and Steel Moment Frame Structures." *Jo. Struct. Eng. ASCE*, **130**(2), 361-367.
- Fargier-Gabaldon, L.B. and Parra-Montesinos, G.J. (2006), "Behavior of reinforced concrete column-steel beam roof level T-connections under displacement reversals." *J. Struct. Eng. ASCE*, **132**(7), 1041-1051.
- Goel, S.C. (2004), "United States-Japan Cooperative Earthquake Engineering Research Program on Composite and Hybrid Structures." *J. Struct. Eng. ASCE*, **130**(2), 157-158.
- Han, L.H. (2002), "Tests on stub columns of concrete-filled RHS sections." *J. Const. Steel Res.*, **58**(3), 353-372.
- Hadianfard, M.A. and Rahnama H. (2010). "Effects of RHS face deformation on the rigidity of beam-column connection." *Steel. Comp. Struct.*, **10**(6), 489-500.
- Hwang, S.-K. and Yun, H.-D. (2004), "Effects of transverse reinforcement on flexural behaviour of high-strength concrete columns." *Eng. Struct.*, **26**(1), 1-12.
- Jiang W.S. and Bai G.L. (1994), "Seismic behavior and Seismic design of short concrete column reinforced by compound hoops, spiral stirrups and X-shaped bars." *J. Building. Struct.*, **15**, 14.(in Chinese)
- Kanno, R. and Deierlein, G.G. (2000), "Design Model of Joints for RCS Frames." Design Model Of Joints For Rcs Frames. *Composite Construction in Steel and Concrete IV-Proceedings of the United Engineering Foundation Conference*, Banff, Alberta, Canada, 947-958.
- Kuramoto, H. and Nishiyama, I. (2004), "Seismic Performance and Stress Transferring Mechanism of Through-Column-Type Joints for Composite Reinforced Concrete and Steel Frames." *J. Struct. Eng. ASCE*, **130**(2), 352-360.
- Liang, X.M. and Parra-Montesinos, G.J. (2004), "Seismic behavior of reinforced concrete column-steel beam subassemblies and frame systems." *J. Struct. Eng. ASCE*, **130**(2), 310-319.
- Liu, J. and Astaneh-Asl, A. (2000), "Cyclic behavior of steel shear connections with floor slab." *Comp. Hybrid. Struct.*, **1-2**, 745-752.
- Minami. (1994), "The elastic and plastic behaviour of the long shank high strength bolted connection in the hybrid structure consisting of steel beam and concrete column." *Annual. Symposium. Con. Struct. Architectural. Ins. Japan.*, **16**, 2. (in Japanese)
- Nishiyama, I., Kuramoto, H. and Noguchi, H. (2004), "Guidelines: Seismic design of composite reinforced concrete and steel buildings." *J. Struct. Eng. ASCE*, **130**(2), 336-342.
- Noguchi, H. and Uchida, K. (2004), "Finite element method analysis of hybrid structural frames with reinforced concrete columns and steel beams." *J. Struct. Eng. ASCE*, **130**(2), 328-335.
- Parra-Montesinos, G. and Wight, J.K. (2000), "Seismic response of exterior RC column-to-steel beam connections." *J. Struct. Eng. ASCE*, **126**(10), 1113-1121.
- Parra-Montesinos, G.J., Liang, X. and Wight, J.K. (2003), "Towards deformation-based capacity design of RCS beam-to-column connections." *Eng. Struct.*, **25**(5), 681-690.
- Shibata, M., Nakazawa, A., Mihara, J., Masuo, K. and Minami, K. (1992), "Development of a Specially Designed High-Strength Transverse Reinforcement for Square Concrete Columns." *Proce. Tenth. World. Conference. Earthq. Eng.*, Madrid, Spain, July, *1-10*, 3065-3070.
- Xiao, Y. and Martirosyan, A. (1998), "Seismic Performance of High-Strength Concrete Columns." *J. Struct. Eng.*, **124**(3), 241-251.